



HAL
open science

Heteroepitaxial Growth of Lithium Niobate Thin Films on Sapphire Substrates with Different Orientations by Pulsed-Laser Deposition

Ihor Pershukov, Jérôme Richey, Emma Borel, Elisa Soulat, Marie Bousquet, Florian Dupont, Bertrand Vilquin

► **To cite this version:**

Ihor Pershukov, Jérôme Richey, Emma Borel, Elisa Soulat, Marie Bousquet, et al.. Heteroepitaxial Growth of Lithium Niobate Thin Films on Sapphire Substrates with Different Orientations by Pulsed-Laser Deposition. 2022 IEEE International Symposium on Applications of Ferroelectrics (ISAF 2022), IEEE, Jun 2022, Tours, France. 10.1109/ISAF51494.2022.9870044 . hal-03715485

HAL Id: hal-03715485

<https://hal.science/hal-03715485>

Submitted on 21 Mar 2023

HAL is a multi-disciplinary open access archive for the deposit and dissemination of scientific research documents, whether they are published or not. The documents may come from teaching and research institutions in France or abroad, or from public or private research centers.

L'archive ouverte pluridisciplinaire **HAL**, est destinée au dépôt et à la diffusion de documents scientifiques de niveau recherche, publiés ou non, émanant des établissements d'enseignement et de recherche français ou étrangers, des laboratoires publics ou privés.

Heteroepitaxial growth of Lithium Niobate Thin Films on sapphire substrates with different orientations by Pulsed-Laser Deposition

Ihor Pershukov^{1,2}, Jérôme Richy¹, Emma Borel¹, Elisa Soulat¹, Marie Bousquet¹, Florian Dupont¹, Bertrand Vilquin²

¹ Univ. Grenoble Alpes, CEA-LETI MINATEC-CAMPUS, 38000, France, ihor.pershukov@cea.fr;

² Univ Lyon, Ecole Centrale de Lyon, Université Claude Bernard Lyon 1, CPE Lyon, INSA Lyon, CNRS, INL UMR5270, 69130 Ecully, France

Abstract— In this study, epitaxial LiNbO₃ thin films were successfully grown on *a*- and *c*-Al₂O₃ substrates by Pulsed Laser Deposition (PLD). In order to control the film crystallinity and chemical composition, the influence of different growth parameters, such as substrate temperature, oxygen pressure, and target composition, were studied. The physical and chemical properties of the as-deposited LiNbO₃ layers were characterized.

Keywords — pulsed laser deposition, ferroelectric thin film, lithium niobate, epitaxy.

I. INTRODUCTION

With the deployment of the fifth generation of mobile communications (5G) and the Internet of Things, radiofrequency (RF) filters performances have to be improved. Nowadays, RF filters are mainly based on acoustic resonators such as Surface Acoustic Waves (SAW) and Bulk Acoustic Wave (BAW) resonators [1]. Thanks to their high electromechanical coupling coefficient (from 5.6% to 45.8% for bulk waves, depending on the crystalline orientation) and large acoustic velocity (from 3488 to 4750 m/s), single-crystal LiNbO₃ or LiTaO₃ layers are widely used in these applications [2].

LiNbO₃ is a piezoelectric material with a trigonal crystal structure (R3c space group), a Curie temperature around 1200 at near-stoichiometric compositions, low transmission loss, and high stability [3, 4].

Despite LiNbO₃ being known for more than 40 years, no growth technique has yet demonstrated layers with sufficient physical performances for practical use in optical or acoustic devices [4]. Indeed single-phased LiNbO₃ films are notoriously difficult to grow due to their lack of line composition, which makes the chemical composition control difficult. Li volatility is also an important factor to be taken into account. Another difficulty in the growth of this material lies in its high thermal expansion coefficient (TEC α_a is 14.1 10⁻⁶ (K⁻¹) at 300 K) which can cause the presence of cracks [4]. As the natural growth orientation is along the *c*-axis, pure epitaxial growth along with specific directions (e.g. (1 1 0)) compatible with device specifications is also hard to be performed [2, 5]. Congruent composition of LiNbO₃ is nonstoichiometric (48.38 mol% of Li₂O). The physical and structural properties of LiNbO₃ are dependent on the amount of Li in the film. For example, elastic constants, electromechanical coupling (k^2), acoustic velocity, and refractive index, are highly dependent on the Li content of the film. So, for large-scale production of devices, it is necessary to precisely control the chemical composition [2, 6].

LiNbO₃ films are usually crystallized at substrate temperatures of 500-800°C [6, 7, 8]. Due to the high temperature of the deposition and high probability of growth mixes of LiNbO₃ with either Li₃NbO₄ or LiNb₃O₈ that represent centrosymmetric and hence non-ferroelectric phases, achieving the growth of stoichiometric LiNbO₃ thin films is challenging [4, 9].

In the litterature, lithium niobate films were grown epitaxially on *c*-Al₂O₃ substrate using a thermal chemical vapor deposition method from the metalorganic compounds Li(C₁₁H₁₉O₂) and Nb(OC₂H₅)₅, in other words, by MOCVD[10]. Epitaxial LiNbO₃ thin (110) and (001) films were deposited on 10×10 mm² *a*-plane sapphire (Al₂O₃) and 12×7 mm² *c*-plane sapphire (Al₂O₃) substrates by Pulsed Laser Deposition (PLD) [11-12]. It was found that during the PLD process lower oxygen pressure (0.133 mbar) favors *a*-oriented LiNbO₃ film growth while higher oxygen pressure (0.667 mbar) favors *c*-oriented growth [13].

In this article, LiNbO₃ thin films have been deposited by Pulsed laser deposition (PLD) on *c*- and *a*-Al₂O₃ substrates at 500 and 600°C. The atmosphere of oxygen (O₂) with pressures of 0.007 and 0.2 mbar was used during the growth. In order to compensate a potential Li loss during PLD process, different targets were used: LiNbO₃ and LiNbO₃ with an additional 10% of Li₂O. Dependences of the characteristics of the films on substrate orientation, pressure, temperature, and amount of Li in the target were studied.

This paper is organized as follows. The film growth process is described in Section II, and characterizations of the surface morphology and structural properties are shown in Section III. Finally, conclusions are presented in Section IV.

II. EXPERIMENTAL PROCEDURE

The PLD system used in this study is a wafer-based PLD reactor made by Solmates. Laser ablation was done with a KrF excimer laser operating at 248 nm, with a repetition rate of 100 Hz and a laser fluence of 2.1 J/cm². The target-substrate distance was 55 mm. Two targets with different compositions, namely a stoichiometric (LiNbO₃) and a Li-enriched (10% of Li added to LiNbO₃) were used to study the dependence of the films on the amount of Li atoms in the target. 4-inch *c*- and *a*-Al₂O₃ wafers were chosen as substrates since their structure is compatible with LiNbO₃. Two different oxygen pressures have been used in LiNbO₃ film deposition on *c*- and *a*-sapphire substrates, i.e., 0.2 mbar and 0.007 mbar. The deposition temperatures were 500°C and 600°C. Finally, combinations of deposition parameters are summarized in Table I.

TABLE I. DEPOSITION PARAMETERS USED FOR LiNbO_3 GROWTH ON SAPPHIRE SUBSTRATES

Substrate orientation	Pressure (mbar)	Deposition temperature ($^{\circ}\text{C}$)	Target
c- Al_2O_3	0.2	500	LiNbO_3
c- Al_2O_3	0.007	500	LiNbO_3
c- Al_2O_3	0.2	600	LiNbO_3
c- Al_2O_3	0.2	600	$\text{Li}_{1.1}\text{NbO}_{3.05}$
c- Al_2O_3	0.007	500	$\text{Li}_{1.1}\text{NbO}_{3.05}$
a- Al_2O_3	0.2	500	LiNbO_3
a- Al_2O_3	0.007	500	LiNbO_3
a- Al_2O_3	0.2	600	LiNbO_3
a- Al_2O_3	0.2	600	$\text{Li}_{1.1}\text{NbO}_{3.05}$
a- Al_2O_3	0.007	500	$\text{Li}_{1.1}\text{NbO}_{3.05}$

The growth rate of the films was about 11 nm/min and the film thicknesses are about 200 nm.

The surface morphology of LiNbO_3 films was studied by both Scanning Electron Microscopy (SEM) and Atomic Force Microscopy (AFM). X-Ray Diffraction (XRD) in different configurations (θ - 2θ scan, ω scan, ϕ scan) was used to investigate the microstructural properties of the as-deposited LiNbO_3 layers.

III. RESULTS

A. LiNbO_3 films grown on c- Al_2O_3 substrate

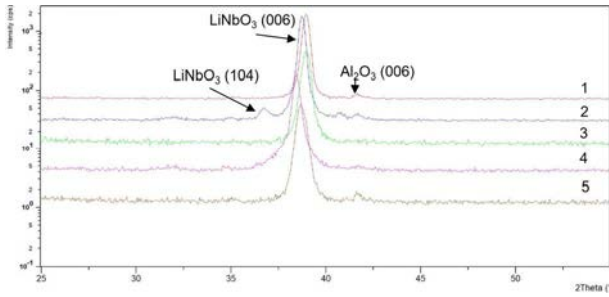


Fig. 1. $\theta/2\theta$ XRD pattern of the LiNbO_3 c-sapphire heterostructure grown at: (1) 0.2 mbar, 500 $^{\circ}\text{C}$, LiNbO_3 target; (2) 0.007 mbar, 500 $^{\circ}\text{C}$, LiNbO_3 target; (3) 0.2 mbar, 600 $^{\circ}\text{C}$, LiNbO_3 target; (4) 0.2 mbar, 600 $^{\circ}\text{C}$, $\text{Li}+\text{LiNbO}_3$ target; (5) 0.007 mbar, 500 $^{\circ}\text{C}$, $\text{Li}+\text{LiNbO}_3$ target.

XRD patterns reveal that LiNbO_3 films grown on c-sapphire show a strong (0 0 1) texture (Fig. 1). The film are single-phased and no parasitic phase (such as Li_3NbO_4 and LiNb_3O_8) was observed. The film grown at 500 $^{\circ}\text{C}$ with the 0.007 mbar O_2 pressure and LiNbO_3 target is the only sample showing also (1 0 4) orientation, but still preferred texturation remains (0 0 6).

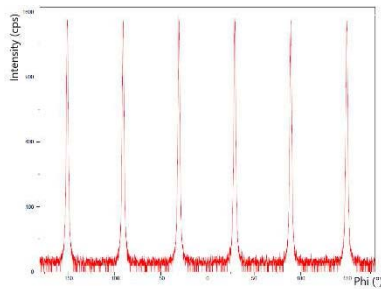


Fig. 2. ϕ -scan LiNbO_3 c-sapphire heterostructure grown at 0.2 mbar, 600 $^{\circ}\text{C}$, LiNbO_3 target performed on LiNbO_3 (0 0 6).

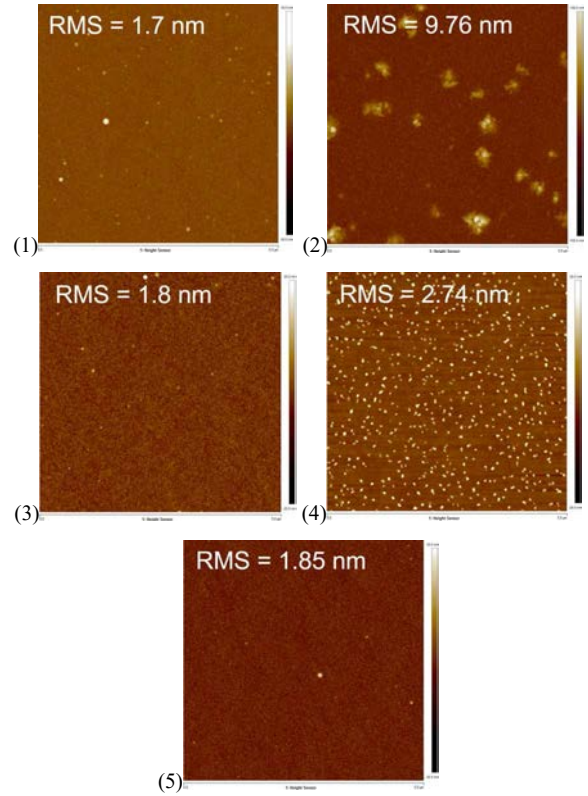


Fig. 3. AFM micrographs of LiNbO_3 films deposited on c- Al_2O_3 substrates grown at different conditions: (1) 0.2 mbar, 500 $^{\circ}\text{C}$, LiNbO_3 target; (2) 0.007 mbar, 500 $^{\circ}\text{C}$, LiNbO_3 target; (3) 0.2 mbar, 600 $^{\circ}\text{C}$, LiNbO_3 target; (4) 0.2 mbar, 600 $^{\circ}\text{C}$, $\text{Li}+\text{LiNbO}_3$ target; (5) 0.007 mbar, 500 $^{\circ}\text{C}$, $\text{Li}+\text{LiNbO}_3$ target. Scan size: (5 \times 5) μm^2 .

Full Width at Half Maximum (FWHM) of LiNbO_3 (0 0 6) peak obtained through symmetric ω -scans is $\sim 0.8^{\circ}$, through asymmetric ω -scans in between ~ 1.6 - 2.1° for (0 1 2). All ϕ -scans (for example, Fig. 2) are having 6-fold symmetry confirming the epitaxial nature of all the samples.

The surface morphology of pulsed laser deposited LiNbO_3 films was investigated by AFM measurements as shown in Fig. 3. Layers consisting of rounded grains can be seen whatever growth conditions. Little particles such as droplets are present in all cases.

As it is seen, the sample deposited at 0.007 mbar, 500 $^{\circ}\text{C}$, with LiNbO_3 target has the highest root mean square (RMS) roughness, around 10 nm, which can be connected to coexistence of (001) and (104) orientations. For other samples surface of the layers is quite smooth with much lower roughness (~ 2 nm), but lower roughness (~ 1 nm) was already reported for z-cut of LiNbO_3 [2]. SEM micrographs (Fig. 4.) confirm the low surface roughness of the films and the absence of the cracks.

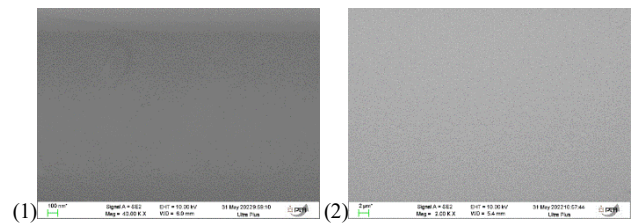


Fig. 4. SEM micrographs of LiNbO_3 c- Al_2O_3 heterostructures grown at: (1) 0.2 mbar, 500 $^{\circ}\text{C}$, LiNbO_3 target; (2) 0.2 mbar, 600 $^{\circ}\text{C}$, LiNbO_3 target.

B. LiNbO_3 films grown on $a\text{-Al}_2\text{O}_3$ substrate

Structural properties of the film were found to be greatly affected by the substrate orientation. Fig. 4 depicts the $\theta/2\theta$ -XRD patterns from a LiNbO_3 film when crystallization occurred during deposition on the $a\text{-Al}_2\text{O}_3$ substrates. In contrast to what was previously observed for LiNbO_3 films deposited on $c\text{-Al}_2\text{O}_3$ (Fig. 4), a growth competition between (006) and (110) are systematically present (Fig. 5).

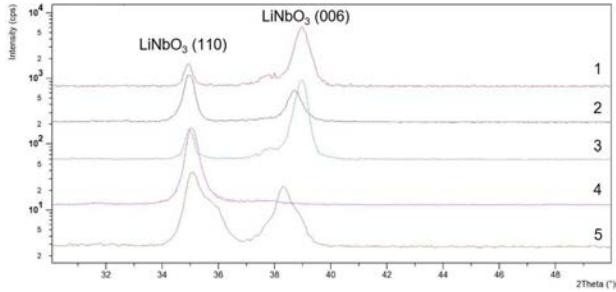


Fig. 5. $\theta/2\theta$ XRD spectra of the LiNbO_3 a -sapphire heterostructure grown at: (1) 0.2 mbar, 500°C, LiNbO_3 target; (2) 0.007 mbar, 500°C, LiNbO_3 target; (3) 0.2 mbar, 600°C, LiNbO_3 target; (4) 0.2 mbar, 600°C, $\text{Li}+\text{LiNbO}_3$ target; (5) 0.007 mbar, 500°C, $\text{Li}+\text{LiNbO}_3$ target.

XRD pattern reveals that LiNbO_3 film deposited on a -sapphire at 600°C, under 0.2 mbar O_2 atmosphere with the help of additional Li in the target is polycrystalline, with strong (1 1 0) texturation. Interesting is also the combination of both (0 0 6) and (1 1 0) orientations were grown on x -cut sapphire also with additional Li in the target, at 500°C with the 0.007 mbar O_2 atmosphere. This indicates that nucleation at the point of solid-phase crystallization does not result in an ideal selection of the (1 1 0) orientation, although (1 1 0) is the major domain in the first growth stage, crystallization has selectivity to c -axis orientation.

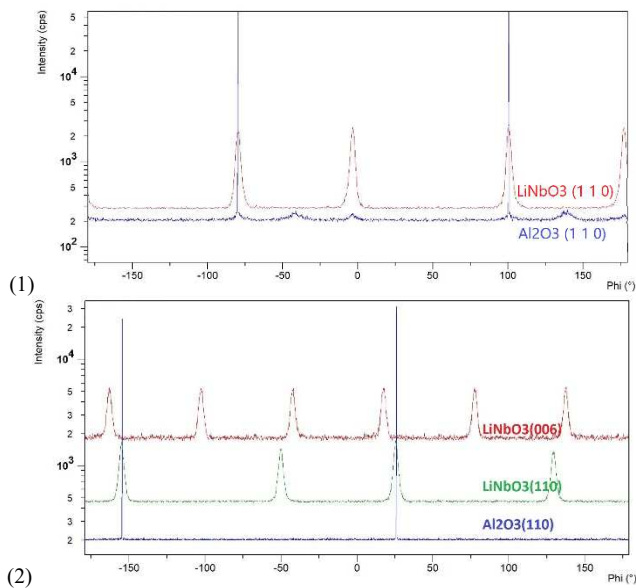


Fig. 6. ϕ -scans of the LiNbO_3 a -sapphire heterostructures grown with $\text{Li}+\text{LiNbO}_3$ target at: (1) 0.2 mbar, 600°C; (2) 0.007 mbar, 500°C.

All ϕ -scans of samples grown with LiNbO_3 target on the x -cut sapphire (not shown there) are having 6-fold symmetry confirming the epitaxial nature of the (0 0 1) layers. In Fig. 5 ϕ -scans of the $\text{LiNbO}_3/c\text{-Al}_2\text{O}_3$ heterostructures grown with additional Li. The sample deposited at 600°C is having only (1 1 0) LiNbO_3 grown. Heterostructure grown at low pressure with 10% of Li added to LiNbO_3 target is having both epitaxial (0 0 1) and (1 1 0) oriented crystals in the film, which also confirms selectivity to c -axis orientation.

Full Width at Half Maximum (FWHM) of LiNbO_3 (0 0 6) peaks grown with unenriched target obtained through symmetric ω -scans are $\sim 0.9^\circ$ - 1.7° , through asymmetric ω -scans in between ~ 2.0 - 2.6° . The same indicators of heterostructure grown at low pressure with 10% of Li added to the LiNbO_3 target are $\sim 1.2^\circ$ and $\sim 2.2^\circ$, respectively. Finally, for epitaxial LiNbO_3 (1 1 0) grown at 600°C, FWHM obtained through symmetric and asymmetric ω -scans are $\sim 1.5^\circ$ and $\sim 1.9^\circ$, respectively.

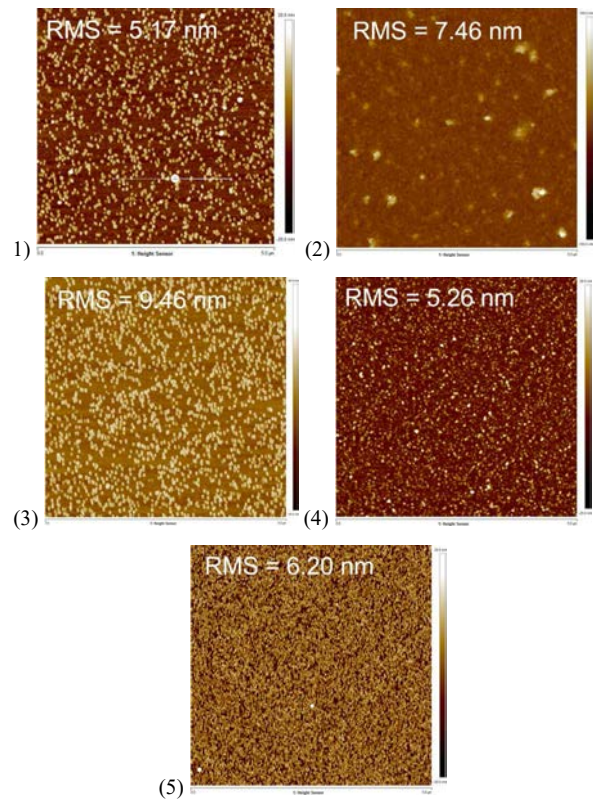


Fig. 7. AFM micrographs of LiNbO_3 films deposited on $a\text{-Al}_2\text{O}_3$ substrates grown at: (1) 0.2 mbar, 500°C, LiNbO_3 target; (2) 0.007 mbar, 500°C, LiNbO_3 target; (3) 0.2 mbar, 600°C, LiNbO_3 target; (4) 0.2 mbar, 600°C, $\text{Li}+\text{LiNbO}_3$ target; (5) 0.007 mbar, 500°C, $\text{Li}+\text{LiNbO}_3$ target. Scan size: $(5 \times 5) \mu\text{m}^2$.

The surface morphology of LiNbO_3 films grown on $a\text{-Al}_2\text{O}_3$ substrate was also investigated with AFM measurements as shown in Fig. 6. Compared to lithium niobate grown on $c\text{-Al}_2\text{O}_3$, layers are also consisting of grains that can be seen in each sample but the number of particles on the surface is much bigger. Root mean square (RMS) roughness is also bigger in comparison to deposition on z -cut. Interestingly, the LiNbO_3 film presenting the (1 1 0) epitaxial layer, *i.e.* film deposited at 600°C from a Li-enriched target, shows the least rough surface.

IV. CONCLUSIONS

In this work, LiNbO₃ thin films have been grown on 4-inch sapphire wafers in a wafer-based PLD reactor with film thicknesses of about 200 nm. The influence of different growth parameters, such as substrate orientation, temperature, oxygen pressure, and target composition, were studied. Single-phased films without parasitic phases (such as Li₃NbO₄ and LiNb₃O₈) were observed.

Epitaxial, single-phase lithium niobate films with *c*-axis and *a*-axis orientations have been deposited and characterized. Predominant orientation toward the *c*-axis was shown. The conditions for LiNbO₃ film growth on *a*- and *c*-Al₂O₃ substrates have been clarified. The *a*-axis orientation of LiNbO₃ thin film on *a*-Al₂O₃ was achieved through the deposition with the help of an additional 10% of Li in the LiNbO₃ target and at 600°C substrate temperature. The possibility of growth of LiNbO₃/Al₂O₃ heterostructures with both epitaxial (0 0 1) and (1 1 0) oriented crystals in the film same time was shown. Future work will be devoted to the integration of the LiNbO₃/Al₂O₃ heterostructure in Surface Acoustic Wave device.

REFERENCES

- [1] R. Aigner, G. Fattinger, M. Schaefer, K. Karnati, R. Rothmund, and F. Dumont, "BAW Filters for 5G Bands," IEEE International Electron Devices Meeting (IEDM), 2018. doi: 10.1109/IEDM.2018.8614564.
- [2] A. Bartasyte, S. Margueron, T. Baron, S. Oliveri, and P. Boulet, "Toward High-Quality Epitaxial LiNbO₃ and LiTaO₃ Thin Films for Acoustic and Optical Applications," Adv. Mater. Interfaces, vol. 4, art. no. 1600998, 2017. doi: 10.1002/admi.201600998.
- [3] M. A. Mohammad, X. Chen, Q.-Y. Xie, B. Liu, J. Conway, H. Tian, Y. Yang, and T.-L. Ren, "Super High Frequency Lithium Niobate Surface Acoustic Wave Transducers up to 14 GHz," in IEEE International Electron Devices Meeting (IEDM), 2015. doi: 10.1109/IEDM.2015.7409729.
- [4] T. Volk and M. Wöhlecke, "Lithium Niobate: Defects, Photorefractive and Ferroelectric Switching"; Springer: Berlin/Heidelberg, Germany, 2008; Volume 115
- [5] B. Zivasatienraj, M.B. Tellekamp, and W.A. Doolittle, "Epitaxy of LiNbO₃: Historical Challenges and Recent Success," Crystals, vol. 11, p. 397, 2021. doi: 10.3390/cryst11040397.
- [6] G. Balestrino *et al.*, "Epitaxial LiNbO₃ thin films grown by pulsed laser deposition for optical waveguides," Appl. Phys. Lett., vol. 78, pp. 1204–1206, 2001. doi: 10.1063/1.1350903.
- [7] A. K. Sarin Kumar *et al.*, "High-frequency surface acoustic wave device based on thin-film piezoelectric interdigital transducers," Appl. Phys. Lett., vol. 85, pp. 1757–1759, 2004. doi: 10.1063/1.1787897.
- [8] T.-H. Lee, F.-T. Hwang, C.-T. Lee, and H.-Y. Lee, "Investigation of LiNbO₃ Thin Films Grown on Si Substrate Using Magnetron Sputter," Mat. Sci. Eng. B, vol. 136, pp. 92-95, 2007. doi: 10.1016/j.mseb.2006.09.001.
- [9] S.-H. Lee, T. K. Song, T. W. Noh, and J.-H. Lee, "Low - temperature growth of epitaxial LiNbO₃ films on sapphire (0001) substrates using pulsed laser deposition," Appl. Phys. Lett., vol. 67, pp. 43-45, 1995, doi: 10.1063/1.115486.
- [10] Y. Akiyama, K. Shitanaka, H. Murakami, Y.-S. Shin, M. Yoshida, and N. Imaishi, "Epitaxial growth of lithium niobate film using metalorganic chemical vapor deposition," Thin Solid Films, vol. 515, pp. 4975–4979, 2007. doi: 10.1016/j.tsf.2006.10.034.
- [11] J. Y. Dai, H. K. Lam, Q. Li, J. Wang, H. L. W. Chan, and C. L. Choy, "Structural characterization and electron-energy-loss spectroscopic study of pulsed laser deposited LiNbO₃ films on a-sapphire," J. Appl. Phys., vol. 96, pp. 6319–6322, 2004. doi: 10.1063/1.1806993.
- [12] Y. Shibata, K. Kaya, K. Akashi, M. Kanai, T. Kawai, and S. Kawai, "Epitaxial growth and surface acoustic wave properties of lithium niobate films grown by pulsed laser deposition," J. Appl. Phys., vol. 77, pp. 1498–1503, 1995. doi: 10.1063/1.358900.
- [13] H. K. Lam, J. Y. Dai, and H. L. W. Chan, "Orientation controllable deposition of LiNbO₃ films on sapphire and diamond substrates for surface acoustic wave device application," J. Cryst. Growth, vol. 268, pp. 144–148, 2004. doi: 10.1016/j.jcrysgro.2004.04.111.